An Empirical Model for the Ignition of Aluminum Particle Clouds Behind Blast Waves

Kaushik Balakrishnan[1,*], Allen L. Kuhl[2], John B. Bell,[1] and Vincent E. Beckner[1]
[1] Lawrence Berkeley National Laboratory, 1 Cyclotron Road, Berkeley, CA 94720
[2] Lawrence Livermore National Laboratory, 7000 East Avenue, Livermore, CA 94551

Abstract

An empirical model for the ignition of aluminum particle clouds is developed and applied to the study of particle ignition and combustion behavior resulting from explosive blast waves. This model incorporates both particle ignition time delay as well as cloud concentration effects on ignition. The total mass of aluminum that burns is found to depend on the model, with shorter ignition delay times resulting in increased burning of the cloud. A new mass-averaged ignition parameter is defined and is observed to serve as a useful parameter to compare cloud ignition behavior. Investigation of this variable reveals that both peak ignition as well as time required to attain peak ignition are sensitive to the model parameters. Overall, this study demonstrates that the new ignition model developed captures effects not included in other combustion models for the investigation of shock-induced ignition of aluminum particle clouds.

1 Introduction

Aluminum is generally added to explosives due to its high energy content, which can release additional energy by afterburning during its explosive dispersal. However, the ensuing two-phase mixture involves the confluence and interplay of various physical phenomena that present several challenges to simulating the behavior. Aluminum, when encased in a shell surrounding a booster explosive charge—termed as a Shock Dispersed Fuel (SDF) charge [1]—has gained recent interest, with robust, adaptive numerical simulations being carried out by Kuhl et al. [2,3]. These studies investigated the turbulent mixing effects in the ensuing fireball, and matched experimental pressure traces and late time mean chamber pressures. Balakrishnan et al. [4, 5] have also carried out simulations using a different numerical strategy and have investigated the dispersion and burning characteristics of the particles. The Al particles were shown to cluster due to their interaction with the fluid mechanic structures in the mixing layer, resulting in preferential ignition of the particles.

Despite the above detailed studies, ignition mechanisms of Al need to be revisited, particularly for Al clouds driven by shock/blast waves. Most ignition models of Al particles in the literature are based only on the criterion of the particle heating up to a certain ignition temperature, after which it burns. However, the applicability of such models for particle clouds may not capture all the combustion physics involved. For instance, shock tube experiments undertaken by Boiko et al. [7, 8] show that Al particle ignition also depends on the mass loading of the cloud. In addition, available ignition delay data from experiments can also be used to model the ignition event of Al particle clouds. To this end, a new ignition model that incorporates these features is developed in this study and the ignition characteristics of Al particle clouds behind explosions is investigated.

This paper is organized as follows: Section 2 presents the numerical formulation used in the present study; Section 3 summarizes the preliminary results and discusses them; the main conclusions drawn in this study are summarized in Section 4.

2 Formulation

The two-phase gasdynamic conservation laws under dilute conditions as formulated by Nigmatulin [9] are considered for the current simulations. Here, both phases, viz., gas and solid, are governed by separate continuum laws, and they interact only through source terms that account for inter-phase mass, momentum and energy transfer.

* Corresponding author: kaushikb@lbl.gov

These governing equations and the inter-phase interaction terms are detailed in Kuhl et al. [2, 3, 10], and are not presented here for brevity. Mixing-controlled combustion is assumed, where both the booster products as well as the evaporated aluminum react with the ambient air to form their respective products. The thermodynamics of these reactive processes, and the associated energy versus temperature profiles are explained in [2, 11].

The new ignition model presented in this study for aluminum particle clouds is based on the works of Korobeinikov et al. [12] and Oran et al. [13], which were originally applied for combustion in gas-phase systems only. In this model, an induction parameter, $f(x,t)$, is defined as follows:

$$f(x,t) = \begin{cases} 0, & initial; \\ 0 \leq f < 1, & pre-ignition; \\ \geq 1, & post-ignition. \end{cases} \tag{1}$$

The evolution equation for $f(x,t)$ is obtained as:

$$\frac{\partial \rho_s f}{\partial t} + \vec{u_s} \cdot \nabla \left(\rho_s f\right) = \frac{\rho_s}{t_{ign}\left(T_g\right)} = \rho_s \, A \, exp\left(\frac{-E_a}{RT_g}\right), \tag{2}$$

where ρ_s is the particle cloud density, u_s is the average particle velocity, T_g is the local gas temperature, R is the universal gas constant, and $t_{ign}(T_g)$ is the ignition time delay of the particles, which is empirically determined based on an Arrhenius-type model, with appropriate choices for the pre-exponential factor, A, and activation energy, E_a. The equation for t_{ign} is assumed to be of the form:

$$\begin{aligned} \frac{1}{t_{ign}(T_g)} &= A_{Kuhl-Boiko} \, exp\left(\frac{-E_{a,Kuhl-Boiko}}{RT_g}\right), \quad T_g \leq 2000K; \\ \frac{1}{t_{ign}(T_g)} &= A \, d_p^2 \, exp\left(\frac{-E_a}{RT_g}\right), \quad T_g > 2000K, \end{aligned} \tag{3}$$

where d_p is the particle diameter. The above constants are computed based on re-shocked aluminum ignition experiments performed by Boiko et al. [7, 8] for ambient gas temperatures $\leq$ 2000 K, and are determined to be $A_{Kuhl-Boiko}$ = 6.25 $\cdot$ 10^{10} sec^{-1} and $E_{a,Kuhl-Boiko}$ = 60 KCal/mol for flake aluminum of size 4–6 μm [14]. For higher ambient gas temperatures, E_a = 22.8 KCal/mol based on Roberts et al. [15] is used. Since A is unknown in the $T_g > 2000$ K limit, different values are considered and its effect on the results are investigated.

The species conservation equations read as:

$$\frac{\partial \rho_g Y_k}{\partial t} + \vec{u_g} \cdot \nabla \left(\rho_g Y_k\right) = \omega_k + \delta_k \cdot \dot{\sigma_s} \cdot \mu_c \left(\rho_s\right), \tag{4}$$

where ρ_g is the gas density, u_g is the gas velocity, Y_k is the mass fraction of the k-th species, with k = fuel, air, products, driver or driver products, and δ_k represents the Kronecker delta, which is 1 when k = fuel, and 0 otherwise. The source term, ω_k, represents the mass production/comsumption per unit volume of the k-th species, and is evaluated assuming a mixing-controlled, infinite chemistry reaction rate. The term $\dot{\sigma_s}$ denotes the inter-phase mass transfer rate, and is obtained using an empirical function of the Reynolds number; this term is included only when k = fuel. For more details, refer to [2, 3]

Past studies have shown that aluminum particle cloud ignition is also determined by its concentration/loading [7, 8, 16]. For too small a particle loading, even though a few particles may ignite, they fail to ignite the cloud, as the particles are far apart and the energy release from the burning particles may not ignite other particles. Thus, a threshold particle loading is required for sustained burning of Al clouds, which has been measured to be 40 g/m^3 by [16], and $\sim$150 g/m^3 by Boiko et al. [7, 8]. In the present study, a cloud ignition probability function, $\mu_c(\rho_s)$, is proposed [14] based on the data from [7, 8], and is computed as

$$\mu_c \left(\rho_s\right) = \frac{1}{1 + exp\left[\left(\rho_s^o - \rho_s\right)/b\right]}. \tag{5}$$

ρ_s^o = 130 g/m^3 and b = 20 are assumed, and μ_c is multiplied to the mass transfer rate, $\dot{\sigma_s}$, thereby accounting for the cloud mass loading.

The governing equations are integrated using high-resolution upwind methods that are higher-order generalizations of Godunov's method with efficient Riemann solvers [17–19]. The Riemann solver for the solid phase continuum is based on Collins et al. [20]. In order to resolve the finer scales in the mixing layer, local Adaptive Mesh Refinement (AMR) is used, based on [21]. The energy-bearing scales that are of preponderance are resolved using this AMR technique, and is consistent with the ILES approach [22]. Recent studies [2, 3] have shown this simulation strategy to be robust and efficient for the problem under study.

3 Preliminary Results and Discussion

Preliminary simulations are carried out for an SDF charge comprised of 0.5 g of a spherical PETN booster charge surrounded by a cylindrical casing of 1 g of aluminum flakes with a thickness of 4–6 μm [2, 3]. The charge is placed at the center of a cubic box of volume 25×25×25 cm^3 (15.6 liters), and free-slip boundary conditions are applied at the walls. The base grid is 80×80×80, with four levels of refinement used at early times to resolve the finer turbulent scales, after which the number of levels are progressively reduced as the scales grow larger. This resolution ($\Delta_4 = 0.2$ mm) suffices for the current problem, as evidenced by comparisons to experiments presented in recent studies [2, 3], albeit without the ignition model. The goal here is to demonstrate the effect of the cloud ignition model on the late time dynamics of Al combustion and turbulent mixing in the fireball.

Adiabatic flame temperatures for Al-air combustion is ∼4300 K. Due to the unavailability of experimental data for Al flakes at gas temperatures higher than 2000 K, different values for A are considered in the range 10^8–10^9 along with the Kuhl-Boiko curve-fit extended beyond $T_g > 2000$ K, and the respective gas temperature field at 70 μsec are presented in Fig. 1. Rayleigh-Taylor instabilities are observed in the fireball, as also previously reported in explosion studies [3–6], owing to the acceleration of a high-density gradient interface. Mushroom-like structures form at the tip of these Rayleigh-Taylor structures due to shear-driven Kelvin-Helmholtz instability. For A greater than a certain cut-off, the resulting maximum fireball temperatures are ∼ 4300 K, typical for Al-air combustion. For $A = 1 \cdot 10^8$, the higher ignition delay results in lower fireball temperatures, with the peak temperature for this case is ∼ 4000 K, and the gas temperature in most regions of the fireball is ∼ 3000 K, which is typical for the combustion of the booster products, i.e., for a hydrocarbon flame. Thus, this study qualitatively shows that a smaller value for A results in less Al burning and concomitantly lower fireball temperatures.

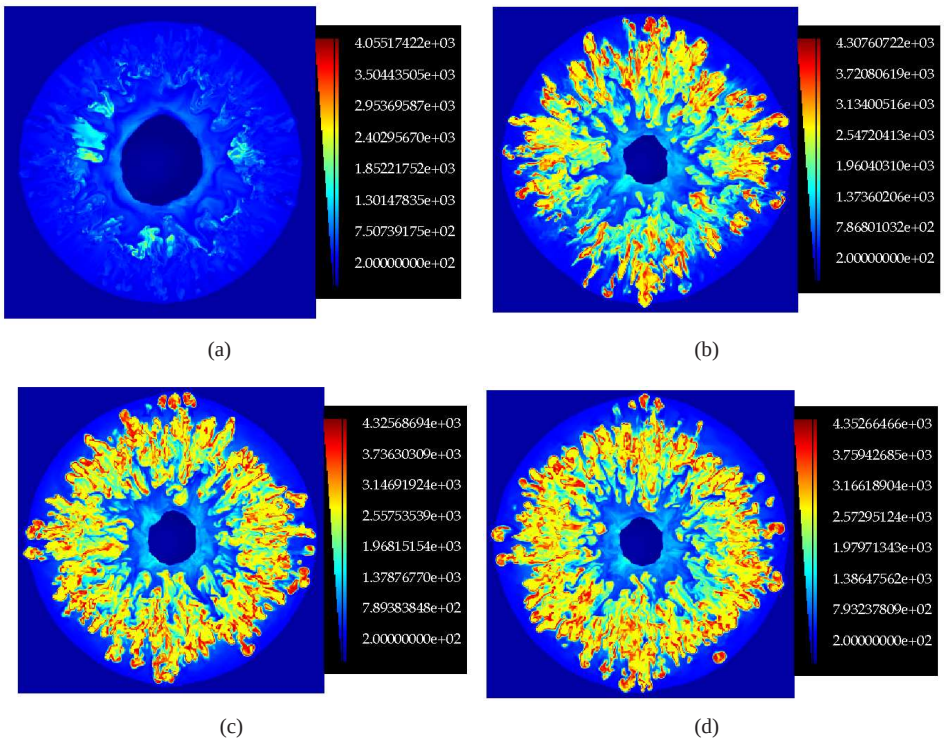

Figure 1: Color scale visualization of a cross-section of the gas temperature field at 70 μsec for different assumed values of A: (a) $1 \cdot 10^8$; (b) $2.5 \cdot 10^8$; (c) $1 \cdot 10^9$; (d) Kuhl-Boiko. The scale denotes the gas temperature in K.

To quantify the above observation, the mass of solid Al remaining (m_{Al}^{solid}) with time is shown in Fig. 2 (a), including also two additional cases corresponding to (i) extending the Kuhl-Boiko [14] curve-fit beyond 2000 K

and (ii) $A \rightarrow \infty$, i.e., $t_{ign} = 0$. For $A = 2.5 \cdot 10^8$, 90% of the Al is consumed; for smaller values of A, which is equivalent to a larger ignition delay, the burning is considerably reduced at late times; as the particle cloud and the fireball expand, relatively less heat is available to sustain the burning and the particles quench. For $A = 1 \cdot 10^8$, since burning is significantly delayed, the particles are allowed to disperse, and the surrounding gases have significantly expanded; consequently, less energy/temperature is available to self-sustain Al burning in the cloud. However, for $A = 2.5 \cdot 10^8$, Al ignition is only partially delayed and about half the Al by mass burns before being quenched. The result with the Kuhl-Boiko curve-fit extended beyond 2000 K predicts a burning trend similar to that with $A = 1 \cdot 10^9$, exemplifying that the induction time delay introduced by the ignition model has almost no role on the burning characteristics of the particles for $A > 5 \cdot 10^8$ and for the Kuhl-Boiko cases; for these cases, the Al burning will be limited by the availability of oxidizer and the heat transfer rate from the gas to the particles. As expected, the Al burning trend for $t_{ign} = 0$ predicts the highest burning rates. This study demonstrates that Al ignition delay times directly impact overall burning trends. From Fig. 2 (a), the model predicts about 90% of Al burns in the confined explosion, which is similar to past experimental results [1], albeit for a different chamber volume. These results also exemplify that the model predictions are in the expected burning trends.

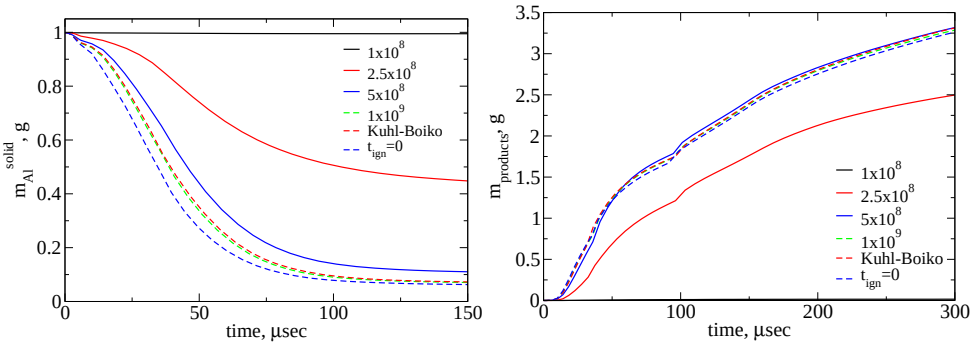

(a) (b)

Figure 2: Mass of (a) solid Al, (b) Al products remaining with time.

Having demonstrated that aluminum combustion is directly related to the choice of A, the dependence of the mass of Al oxidation products ($m_{products}$) on the ignition model is presented in Fig. 2 (b). The trends suggest that less Al products are formed for $A = 1{\times}10^8$ and $2.5{\times}10^8$ as less Al evaporates. For $A = 5{\times}10^8$, even though slightly less Al products are formed by mass compared to the Kuhl-Boiko and t_{ign} =0 cases, at later times, the re-shock effects change the mixing dynamics depending on the amount of Al that has ignited. This re-shock induced mixing can be observed in the form of a slight kink in Fig. 2 (b) near 100 μsec.

Of particular interest in this study is to understand the propagation of the ignition kernel, i.e., the propagation of the ignition front as the particles disperse outward. To this end, the countour of f is presented at 18 μsec for the case with A = $1{\cdot}10^9$ in Fig. 3 (a). The ignition front is observed to be clustered in shape around the Rayleigh-Taylor structures in the mixing layer, and the white circled region from Fig. 3 (a) is magnified and presented in Fig. 3 (b), showing the corrugated/twisted ignition front. It has been recently shown in a different study that particles cluster as they disperse due to their interaction with the vortex rings [5]. This inevitably results in the ignition front to also obtain a twisted shape, thereby increasing the overall surface area of the flame front. Regions with $f \sim 0.5$ are also observed, illustrating that not all regions of the particle cloud ignite to the same intensity. Analysis shows that there are $\sim$32 fine cells across the ignition zone in Fig. 3, so the ignition zone is well resolved by the AMR technique.

These observations are now quantified with the study of a mass-averaged ignition variable, denoted as f_{mass}, which we define as:

$$f_{mass} = \frac{\int \rho_s f dV}{\int \rho_s dV}, \tag{6}$$

where dV denotes a control volume. The variation of f_{mass} with time for the different cases considered in this study is presented in Fig. 4. f_{mass} rises from zero initially, albeit at different rates for the different cases depending on the choice of A. Around 50–60 μsec, f_{mass} peaks, with the peaks $\sim$1 for higher A. For $A \leq 5{\cdot}10^8$, f_{mass} never tends to unity, indicating that the entire Al cloud cannot burn in a self-sustained fashion and only partial burning occurs. This peak value of f_{mass} could also be used as a measure of particle cloud ignition, with lower peaks occurring for higher ignition delay times. The black dashed line joins the peaks, and shows that peak

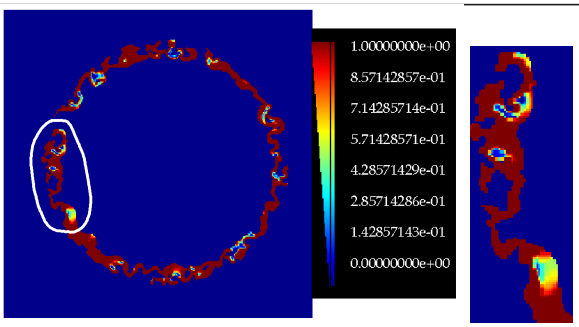

(a) (b)

Figure 3: Color scale visualization of the cross-section of the ignition variable f at 18 μsec for the case with A = $1{\cdot}10^9$. The white circled region from (a) is magnified and presented in (b), showing the corrugated ignition front.

burning occurs earlier for the strongly burning cases; however, the trend shifts between $A = 5{\cdot}10^8$ and $2.5{\cdot}10^8$. Subsequently, as the particles disperse outward and enter relatively cooler regions, f_{mass} gradually decreases. This study illustrates that both peak ignition as well as the time taken to reach peak ignition are dependent on the choice of the ignition model.

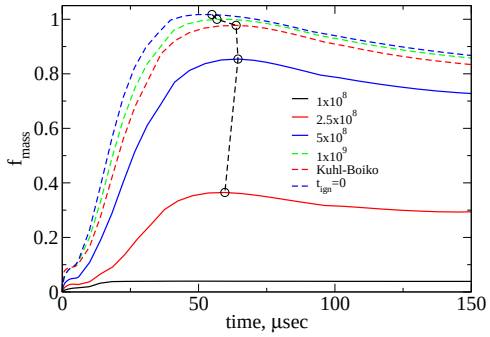

Figure 4: Mass-averaged ignition variable f_{mass} for the different cases considered. The legend denotes the values of A for temperatures higher than 2000 K. The black dashed line joins the peaks.

4 Conclusions

A new empirical model is developed based on experimental data and applied to the investigation of ignition of aluminum particle clouds embedded in explosive blast waves. Effects not previously incorporated in some of the existing models are included in the current developments, and are coupled to the existing adaptive, two-phase numerical simulation strategy. With shorter ignition delay times used in the model, enhanced burning of the cloud occurs. The ignition kernel is distorted in shape due to the interaction of the particles with the vortex rings in the mixing layer. A new mass-averaged ignition parameter is defined and its trends are compared for the different cases considered. Both peak ignition as well as the time required to attain peak ignition are observed to depend on the model parameters. This study demonstrates that the ignition model developed here is useful to the study of aluminum particle cloud ignition and combustion behind explosions.

5 Acknowledgments

This research work was performed under the auspices of the U.S. Department of Energy by the Lawrence Livermore National Laboratory under Contract DE-AC52-07NA27344, and supported by the Defense Threat Reduction Agency. The work at LBNL was performed under contract number DE-FC02-06ER41438. The Simulations were performed at the ERDC High Performance Computing Center.

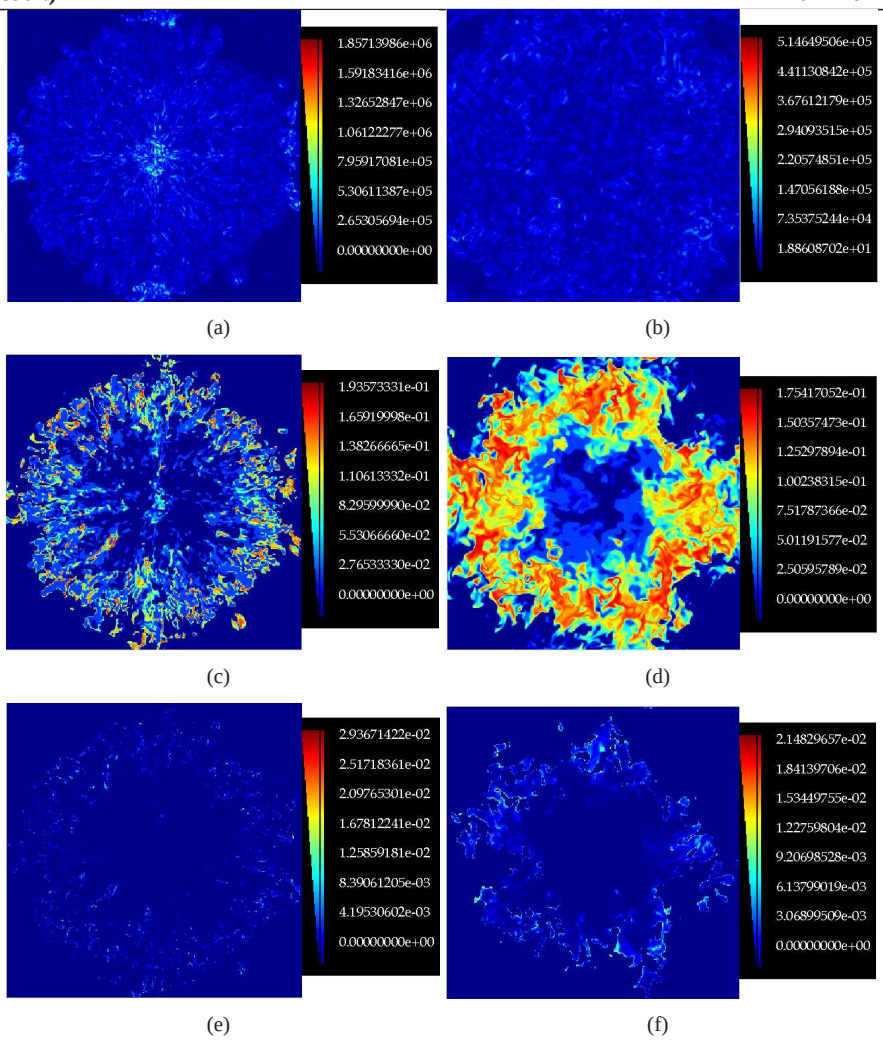

Figure 5: Vorticity (a & b), degree of dissociation (c & d) and degree of ionization (e & f) with the Kuhl-Boiko curve-fit: (a), (c) & (e) at 0.096 msec; (b), (d) & (f) at 0.778 msec.

References

[1] A. L. Kuhl and H. Reichenbach, *Combustion Effects in Confined Explosions*, Proc. Combust. Inst. 32(2) (2009), pp. 2291–2298.

[2] A. L. Kuhl, J. B. Bell and V. E. Beckner, *Heterogeneous Continuum Model of Aluminum Particle Combustion in Explosions*, Combustion, Explosion and Shock Waves 46(4) (2010), pp. 433–448.

[3] A. L. Kuhl, J. B. Bell and V. E. Beckner, *Gasdynamic Model of Turbulent Combustion in TNT Explosions*, 33^{rd} International Combustion Symposium, Beijing, China, August 1–6 (2010).

[4] K. Balakrishnan, and S. Menon, *On the Role of Ambient Reactive Particles in the Mixing and Afterburn Behind Explosive Blast Waves*, Combust. Sci. and Tech. 182(2) (2010), pp. 186–214.

[5] K. Balakrishnan, and S. Menon, *On Turbulent Chemical Explosions Into Dilute Aluminum Particle Clouds*, Combust. Theo. and Model. 14(4) (2010), pp. 583–617.

[6] A. L. Kuhl, *Spherical Mixing Layers in Explosions*, Dynamics of Exothermicity, J. R. Bowen, Ed., Gordon & Breach Publishers, The Netherlands (1996), pp. 291–320 + color plate 4 & 5.

[7] V. M. Boiko, V. V. Lotov and A. N. Papyrin, *Ignition of Gas Suspensions of Metallic Powders in Reflected Shock Waves*, Combustion, Explosion and Shock Waves 25(2) (1989), pp. 193–199.

[8] V. M. Boiko and S. V. Poplavski, *Self-Ignition and Ignition of Aluminum Powders in Shock Waves*, Shock Waves 11(4) (2002), pp. 289–295.

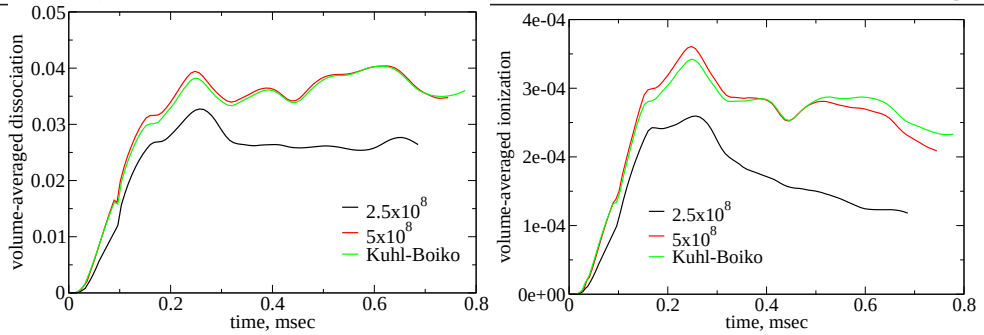

Figure 6: Volume averaged degrees of dissociation and ionization.

[9] R. I. Nigmatulin, *Dynamics of Multiphase Media, Part I*, Hemisphere, New York (1991).

[10] B. Khasainov, A. L. Kuhl, S. Victorov and P. Neuwald, *Model of Non-Premixed Combustion of Al-Air Mixtures*, Proc. 14th APS Meeting on Shock Compression in Condensed Matter 845(1) (2005), pp. 449–452.

[11] A. L. Kuhl and B. Khasainov, *Quadratic Model of Thermodynamic States in SDF Explosions*, 38^{th} Int. Conf. of ICT Energetic Materials, June 26–29 (2007), Karlstruhe, Germany.

[12] V. P. Korobeinikov, V. A. Levin, V. V. Markov and G. G. Chernyi, *Propagation of Blast Waves in a Combustible Gas*, Astronautica Acta 17 (1972), pp. 529–537.

[13] E. S. Oran, J. P. Boris, T. R. Young, M. Flanigan and M. Picone, *Simulation of Gas Phase Detonations: Introduction of an Induction Parameter Model*, NRL Memorandum Report 4255 (1980).

[14] A. L. Kuhl and V. M. Boiko, *Ignition of Aluminum Particles and Clouds*, 41^{st} Int. Conf. of ICT Energetic Materials, June 29–July 2 (2010), Karlstruhe, Germany.

[15] T. A. Roberts, R. L. Burton and H. Krier, *Ignition and Combustion of Aluminum/Magnesium Alloy Particles in O_2 at High Pressures*, Combustion and Flame 92 (1993), pp. 125–143.

[16] R. B. Mason and C. S. Taylor, *Explosion of Aluminum Powder Dust Clouds*, Ind. Eng. Chem. 29(6)(1937), pp. 626–631.

[17] P. Colella and H. M. Glaz, *Efficient Solution Algorithms for the Riemann Problem for Real Gases*, J. Comput. Phys. 59 (1985), pp. 264–289.

[18] J. B. Bell, P. Colella and A. Trangenstein, *Higher Order Godunov Methods for General Systems of Hyperbolic Conservation Laws*, J. Comput. Phys. 82(2) (1989), pp. 362–397.

[19] P. Colella, *Multidimensional Upwind Methods for Hyperbolic Conservation Laws*, J. Comput. Phys. 87 (1990), pp. 171–200.

[20] P. Collins, R. E. Ferguson, K. Y. Chien, A. L. Kuhl, J. Krispin and H. M. Glaz, *Simulation of Shock-Induced Dusty Gas Flows Using Various Models*, AIAA Fluid Dynamics Conference (1994), AIAA 94-2309.

[21] M. J. Berger and P. Colella, *Local Adaptive Mesh Refinement for Shock Hydrodynamics*, J. Comput. Phys. 82(1) (1989), pp. 64–84.

[22] F. F. Grinstein, L. G. Margolin and W. J. Rider (Editors), *Implicit Large-Eddy Simulation: Computing Turbulent Fluid Dynamics*, Cambridge Univ. Press, Cambridge, UK (2007).